

# Modeling and Simulation of Tubular Steam Methane Reformer

Shing-Cheng Chang\*, Tzu-Hsuan Feng\*\*, Cheng-Hao Yang\*.\*.\*  
and Cha'o-Kuang Chen\*\*

**Keywords** : Steam Methane reforming; Porous Catalysts; Hydrogen Generation; Computational Fluid Dynamics..

## ABSTRACT

Steam methane reforming is a major hydrogen production process to convert the methane-rich hydrocarbon-containing gases into hydrogen. This paper presents the numerical model of a tubular steam methane reformer. By solving the mass transport, chemical reactions, and conjugated heat transfer in a double-pipe type of reformer with computational fluid dynamics scheme, the characteristics and performance of steam methane reforming process are investigated. The simulation results are in good agreement with the experimental data as the simulation parameters are adjusted to fit the specific catalysts. In the study cases of the present work, the calculated methane reforming rates are ranged from 63% to 99% with the hydrogen production rate in the range of 62%~87% by the various simulation parameters. It shows that the present numerical model has enough accuracy and is suitable for different catalyst beds for steam methane reforming process.

## INTRODUCTION

To reduce the impact of using fossil fuels to generate heat and power on environment, a more efficient and less polluting utilization of fuel resources was dedicated in recent decades. For example, the biogas from the anaerobic digestion of waste organic substrates is regarded as a potential non-fossil source in the future. By the fuel processing technology, the carbon-hydrogen gas like biogas and natural gas can be reformed into hydrogen rich gases. As the most abundant element on earth, hydrogen has high

capacity of storing energy from primary sources and is nowadays considered the most promising energy vector to be applied in green technologies (Palma et al., 2017). The hydrogen economy focuses on the production of energy from hydrogen, e.g. hydrogen-based fuel cells for power and heat generation. The penetration of advanced and efficient energy fuel cell systems in European Commission EU shows it have the potential for substantially contributing to the decarbonization of the energy system (European Commission EU, Energy Roadmap 2050).

Generating a relatively stable hydrogen rich gas to a fuel cell system is important for stable power supply. Generally, the fuel processors can be carefully designed for different hydrogen rich fuels, such as natural gas, propane, gasoline, diesel, methanol/ethanol and bio-fuels. Among these useful fuels for hydrogen generation, the well distributed natural gas is one of the preferred fuels (Lee et al., 2005). The major hydrogen production process for convert the methane-rich hydrocarbon-containing gases into hydrogen and carbon oxides is the steam methane reforming, which needs a high reaction temperature and is generally operated above 753 K (Peng, 2012).

The steam methane reforming is a highly endothermic reaction process. In the reforming process, the fuel gas to be reformed is premixed along with steam to the reformer tubes filled with catalysts. The steam methane reforming is generally accompanied with the water gas shift reaction which converts CO, the production of steam methane reforming, and steam to form H<sub>2</sub> and CO<sub>2</sub>. After overall reactions, The producing syngas stream, namely reformat, contains H<sub>2</sub>, CO, CO<sub>2</sub>, and unconverted CH<sub>4</sub> and residual steam.

The steam methane reforming includes not only chemical reactions but also significant heat and mass transfer. The process optimization can be achieved by numerical simulation with parametric optimization for mass and energy management. Fukuhara and Igarashi (2005) developed a two-dimensional model to analyze the operation of the coupling methanol decomposition and methane combustion. The performance of a wall-type reactor was compared with a fixed bed one, in

*Paper Received September, 2019. Revised October, 2019. Accepted October, 2019. Author for Correspondence: Shing-Cheng Chang.*

*\*Green Energy & Environment Research Laboratories, Industrial Technology Research Institute, Tainan, Taiwan., ROC.*

*\*\* Department of Mechanical Engineering, National Cheng Kung University, Tainan, Taiwan, ROC.*

which the exothermic and endothermic reactions proceeded simultaneously. Mei et al. (2007) numerically studied a multilayered cylindrical metal monolithic reactor. The steam methane reformer with the catalysts were deposited on the channel walls was coupled with combustion of methane to promote the heat transfer on the metal.

Besides the steady phenomena, the dynamic behaviors could be studied as well by using a theoretical model, such as the one-dimensional pseudo-homogeneous plug flow model proposed by Ramaswamy et al. (2008) for steam methane reactors. Whereas, a one dimensional heterogeneous model was adopted by Bayat et al. (2012) to study the performance of two different configurations of a thermally coupled reactor with two-layered cylindrical structure.

The steam methane reformer is attractive in recent years for the combination of fuel cell power systems. Although there has been many experimental and numerical researches for steam methane reactors, some technical bottlenecks are still yet to be solved. Ni et al. (2015) indicated that the reliability of reformer needs to be improved during the frequent startup and shutdown operations. Besides, the relationship between the reactor configuration, the temperature profiles of the catalyst bed and the system efficiency also needs to be investigated in detail.

To reproduce the behavior of the prototype reactor and to simulate its operation, Pret et al. (2015) developed a CFD model that is able to reproduce the behavior of the prototype reactor and to simulate its operation. The calibration and validation of the numerical model was achieved by comparing the results of the simulation with temperatures and gas composition measurements directly obtained from the prototype reactor.

In the present study, the numerical model of steam methane reforming in a tubular catalyst bed is proposed. A double-pipe heat exchanger is adopted as the basic unit of the reformer. By solving the mass transport, heat transfer, and chemical reactions, the performance of the steam methane reformer is investigated by monitoring the spatial temperature distributions and the reformat compositions in the processor. In the study cases, the simulation parameters related to the catalyst characteristics are varied and analyzed. Furthermore, the temperature effect of inlet fuel gases on the producing reformat is investigated.

## METHODOLOGY

### Governing equations

The steam methane reforming process includes heat transfer, mass transportation, and chemical reactions between the input fuel gases of methane and steam, and the output production gases of hydrogen, carbon-monoxide and carbon-dioxide. The governing

equations are modelled and solved by the computational dynamics (Blazek, 2001) in this study as:

#### (1) Continuity equation

The continuity equation of mass conservation is 
$$\frac{\partial \rho}{\partial t} + \frac{\partial}{\partial x_i}(\rho u_i) = 0 \quad (1)$$
 where  $\rho$ ,  $t$  and  $u_i$  are the fluid density, evolution time, and flow velocity at  $i$  direction respectively.

#### (2) Reynolds-averaged Navier–Stokes equations (RANS)

The momentum equation is solved by the Reynolds-averaged Navier–Stokes equations as

$$\begin{aligned} & \frac{\partial \rho}{\partial t}(\rho u_i) + \frac{\partial \rho}{\partial x_j}(\rho u_i u_j) \\ &= -\frac{\partial P}{\partial x_i} + \frac{\partial}{\partial x_j} \left[ \mu \left( \frac{\partial u_i}{\partial x_j} + \frac{\partial u_j}{\partial x_i} - \frac{2}{3} \delta_{ij} \frac{\partial u_l}{\partial x_l} \right) \right] \\ &+ \frac{\partial}{\partial x_j}(-\rho \overline{u_i u_j'}) \end{aligned} \quad (2)$$

where  $p$  is pressure,  $\mu$  is fluid viscosity, and  $\overline{u_i u_j'}$  is the terms of Reynolds stress.

#### (3) The standard k-ε turbulence model

Besides the Reynolds-averaged Navier–Stokes equations, the standard k-ε turbulence model (Jones and Launder, 1972) is introduced to solve the turbulence flow field as,

$$\begin{aligned} & \frac{\partial}{\partial t}(\rho k) + \frac{\partial}{\partial x_i}(\rho k u_i) \\ &= \frac{\partial}{\partial x_j} \left[ \left( \mu + \frac{\mu_t}{\sigma_k} \right) \frac{\partial k}{\partial x_j} \right] + G_k + G_b + -\rho \varepsilon - Y_M + S_k \quad (3) \\ & \frac{\partial}{\partial t}(\rho \varepsilon) + \frac{\partial}{\partial x_i}(\rho \varepsilon u_i) \\ &= \frac{\partial}{\partial x_j} \left[ \left( \mu + \frac{\mu_t}{\sigma_\varepsilon} \right) \frac{\partial \varepsilon}{\partial x_j} \right] + C_{1\varepsilon} \frac{\varepsilon}{k} (G_k + C_{3\varepsilon} G_b) \\ & - C_{2\varepsilon} \rho \frac{\varepsilon^2}{k} + S_\varepsilon \end{aligned} \quad (4)$$

In the equations,  $G_k$  is the turbulent kinetic energy generation term due to the average velocity gradient, and  $G_b$  is the turbulent kinetic energy generation term due to buoyancy. The term  $Y_M$  represents the contribution of the expansion expansion to the overall dissipation rate in the compressible turbulent flow, and  $\mu_t$  is the turbulent flow viscosity defined as,

$$\mu_t = \rho C_\mu \frac{k^2}{\varepsilon} \quad (5)$$

The coefficients,  $\sigma_k$  and  $\sigma_\varepsilon$ , are the turbulent Prandtl number of  $k$  and  $\varepsilon$ , while  $S_k$  and  $S_\varepsilon$  are source terms. The constants  $C_\mu$  is chosen as  $C_{1\varepsilon} = 1.44, C_{2\varepsilon} = 1.92, C_{3\varepsilon} = 0.09, \sigma_k = 1.0, \sigma_\varepsilon = 1.3$  (Launder and Sharma, 1974).

#### (4) The energy equations

$$\begin{aligned} & \frac{\partial}{\partial t}(\rho E) + \frac{\partial}{\partial x_i}[u_i(\rho E + p)] \\ &= \frac{\partial}{\partial x_j} \left[ \left( k + \frac{c_p \mu_t}{Pr_t} \right) \frac{\partial T}{\partial x_j} + u_i(\tau_{ij})_{eff} \right] + S_h \end{aligned} \quad (6)$$

where  $E$  is the total energy,  $c_p$  is the heat capacity under constant pressure,  $T$  is the temperature, and  $S_h$  is the heat source.  $(\tau_{ij})_{eff}$  is the deflection stress tensor defined as

$$(\tau_{ij})_{eff} = \mu_{eff} \left( \frac{\partial u_i}{\partial x_j} + \frac{\partial u_j}{\partial x_i} \right) - \frac{2}{3} \mu_{eff} \frac{\partial u_i}{\partial x_i} \delta_{ij} \quad (7)$$

In this study, the P1 radiation model (Peng, 1964) is adapted as

$$-\nabla \cdot q_r = aG - 4an^2\sigma T^4 \quad (8)$$

where  $q_r$  is heat radiation flux,  $a$  is absorption coefficient,  $G$  is the incident radiation,  $n$  is the refractive index of the medium, and  $\sigma$  is the Boltzmann constant.

#### (5) The Chemical species transmission equation

In this study, the species transport model is used to calculate the chemical reaction part. The  $Y_i$  solution equation for each chemical species needs to be expressed as

$$\frac{\partial}{\partial t}(\rho Y_i) + \frac{\partial}{\partial x_j}(\rho u_j Y_i) = -\frac{\partial J_{ij}}{\partial x_j} + R_i + S_i \quad (9)$$

where  $J_{ij}$  is the diffusive flux of type  $i$ ,  $R_i$  is the net generation rate of  $i$  type due to chemical reaction, and  $S_i$  is the source term. For the turbulence flows, the diffusion flux is defined as (Zel'dovich and Raizer, 2002)

$$J_{ij} = -\left(\rho D_{i,m} + \frac{\mu_t}{Sc_t}\right) \nabla Y_i - D_{T,i} \frac{\nabla T}{T} \quad (10)$$

where  $D_{i,m}$  and  $D_{T,i}$  are the mass diffusion coefficient and thermal diffusion coefficient of the  $i$  type species. the,  $Sc_t$  is the turbulent Schmidt number.

#### (6) Mixture fraction transmission equation

The mixture fraction is defined as (Sivathanu and Faeth, 1990)

$$f = \frac{Z_i - Z_{i,ox}}{Z_{i,fuel} - Z_{i,ox}} \quad (11)$$

Where  $Z_i$  is the mass fraction of the element  $i$ . the subscript  $ox$  represents the value at the oxidant inlet, and the subscript  $fuel$  represents the value at the fuel inlet. The Favre average (density average) mixture fraction formula is

$$\begin{aligned} \frac{\partial}{\partial t}(\rho \bar{f}) + \frac{\partial}{\partial x_i}(\rho u_i \bar{f}) \\ = \frac{\partial}{\partial x_j} \left[ \left( \frac{k}{c_p} + \frac{\mu_t}{\sigma_t} \right) \frac{\partial \bar{f}}{\partial x_j} \right] + S_m \end{aligned} \quad (12)$$

where  $k$  is the laminar heat transfer coefficient of the mixture,  $c_p$  is the specific heat of mixing,  $\sigma_t$  is the Prandtl number, and  $S_m$  is the source term. The mixture fraction variation  $\bar{f}'^2$  can be obtained by (Jones and Whitelaw, 1982)

$$\begin{aligned} \frac{\partial}{\partial t}(\rho \bar{f}'^2) + \frac{\partial}{\partial x_i}(\rho u_i \bar{f}'^2) \\ = \frac{\partial}{\partial x_j} \left[ \left( \frac{k}{c_p} + \frac{\mu_t}{\sigma_t} \right) \frac{\partial \bar{f}'^2}{\partial x_j} \right] + C_g \mu_t \left( \frac{\partial \bar{f}}{\partial x_j} \right)^2 - C_d \rho \frac{\varepsilon}{k} \bar{f}'^2 \end{aligned} \quad (13)$$

where  $f' = f - \bar{f}$ . The constants  $C_t$ ,  $C_g$ ,  $C_d$  are 0.85, 2.86, 2.0 respectively.

#### Simulation model

The present work studies the steam methane reforming process in a tubular reformer filled with Ni-based catalysts coating on  $Al_2O_3$  particles. As shown in Figure. 1, a double-pipe heat exchanger is adopted for the simulation model. The material of pipes is stainless steel. The inner pipe is divided into three parts, including the front cavity for methane-steam mixing gases flowing into the tube, the porous area with filled catalyst particles, and the rear part for producing reforming gases flowing out the tube. Since the steam methane reforming process is an endothermic, a high temperature combustion gas is introduced into the outer pipe to provide the heat needed for the fuel reforming. As shown in Fig. 1, the counter-flow heat exchanger with higher heat exchange efficiency is adopted in the basic study case.

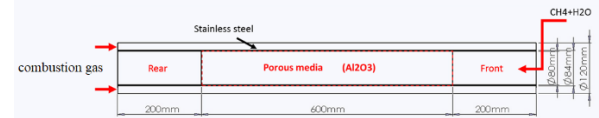


Fig. 1. Simulation of the tubular steam methane reformer.

In this study, a type of commercial Ni-based catalyst is used to transform the methane into hydrogen at high temperature above  $600^\circ\text{C}$ . The catalyst bed is 600mm long with a diameter of 80mm, i.e. the volume of the catalyst bed is 3L. The methane flow rate of inlet is 11.5 normal liter per minute (nlpm). The steam-to-carbon ratio (S/C) is chosen as 3. To make sure the temperature of reforming reaction is high enough, the steam-methane mixing gases is typically pre-heated. In this study, the preheating temperature of the fuel gases is set to three levels of  $500^\circ\text{C}$ ,  $600^\circ\text{C}$  and  $700^\circ\text{C}$  to investigate the effect of fuel inlet temperature on the reforming performance. In the outer pipe of the model, the air flows of 110 nlpm at  $900^\circ\text{C}$  is adopted.

The reforming and exhaust gas outlets are at ambient pressure. The no-slip and no-penetration condition conditions are applied to the solid walls. The adiabatic condition is assumed on the outer surface of the simulation model, while in the interface of inner and outer pipes, the conjugated heat transfer is calculated to ensure the heat needed in the methane reforming process can be provided by the combustion gas.

In this study, the main reaction of the fuel reforming processes are the steam-methane reforming reaction and water-gas-shift reaction as



The reaction rate constant is computed using the modified Arrhenius expression as

$$k = AT^\beta e^{\frac{-E}{RT}} \quad (16)$$

where the dimensionless parameter  $\beta$  is the temperature factor. The activation energy,  $E$ , is set according to the chemical reactions of Eqs. (14) and (15). The parameter  $A$  is the pre-exponential factor of the unit of  $cm^3/(mol \cdot s)$  with relation to the reaction rate. In this study, the effect of the pre-exponential factor on the fuel reforming performance is analyzed.

The species transport and chemical reactions of  $CH_4 \cdot H_2O \cdot H_2 \cdot CO \cdot CO_2$  gases are calculated by using CFD software in the simulation. Simultaneously, the fluid and solid conjugated heat transfer are solved. The radiation effect is included in the simulation by using the P1 radiation model. For the equation of state, the incompressible ideal gas is applied. To solve the turbulent regime of fluid flows, the standard  $k-\epsilon$  turbulence model is adopted. The porous catalyst bed based on aluminum oxide is applied in the simulation by setting the isotropic viscous resistance and inertia resistance of the materials.

## RESULTS AND DISCUSSIONS

### Steam methane reforming in tubular catalyst bed

The present study present the numerical modeling of steam methane reforming. The simulation of reforming process in a tubular catalyst bed is performed. The temperature distribution in the reformer is shown in Figure 2. The temperature of inlet fuel gases is  $600^\circ C$ . In the front area before the fuel gases entering the catalyst bed, the fuel is slightly heated by the combustion gas. As the fuel gases passing through the catalyst bed, the endothermic reforming reaction make a short temperature-discontinuous phenomena on the catalyst interface. As in the section A in Fig. 2, the core temperature of the catalyst bed is less than that of upstream. After the reforming process finished, the reformat is heating to  $724^\circ C$  in this case.

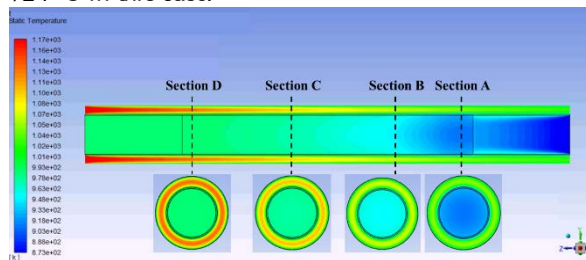


Fig. 2. Temperature distribution of the tubular steam methane reformer.

The thermal gradient between the side wall and the center of the bed is considerable because the steam methane reforming process requires a huge expenditure of energy (Nijemeisland et al., 2004; Shayegan et al., 2008). The radial thermal profiles of the catalytic bed in the upstream, midstream and downstream sections are shown in Fig.2 as well. The simulation results show that the maximum temperature gradient occurs on the reactor walls. The

results are in consistent with the work of Palmaet et al. (2017)

Figure 3 shows the mole fraction distributions of  $CH_4$  and  $H_2$  of the tubular steam methane reformer. In this case, most of methane gases are reformed before the gas flow passing through the middle section of the catalyst pipe. In the fuel gas exit, 93.4% of methane gases are reformed. Finally, the producing dry reformat gas includes 76% mole fraction of hydrogen.

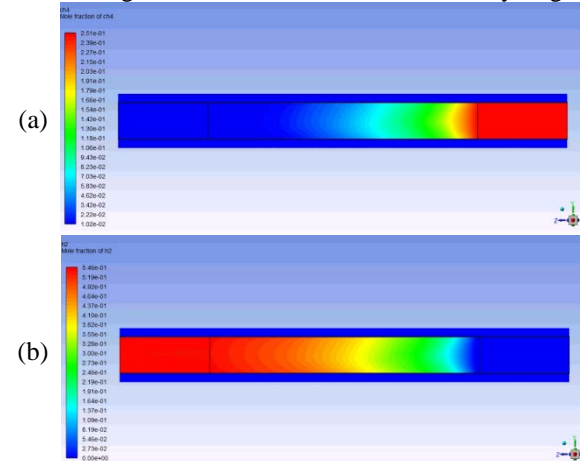


Fig. 3. Mole fraction distribution of (a)  $CH_4$  and (b)  $H_2$  of the tubular steam methane reformer.

To evaluate the hydrogen producing abilities of the reformer, the hydrogen production rate is generally calculated as

$$\eta = \frac{\text{Actual hydrogen production}}{\text{Maximum hydrogen production}} \quad (17)$$

According to Eqs.(14) and (15), the maximum hydrogen production of 1 mole methane reforming is 4 mole hydrogen molecules. In the present case, the hydrogen production rate is 79.48%. Since the methane reforming occurs in a porous catalyst bed, the velocity of the fuel gas is enlarged. Figure 4 shows the flue flow is accelerated in the tubular reformer and then decelerated as the reformat flowing into the rear area. Because the reformat flow rate is larger than the inlet steam-methane mixing gases, the flow velocity in the exit is larger than that of the inlet.

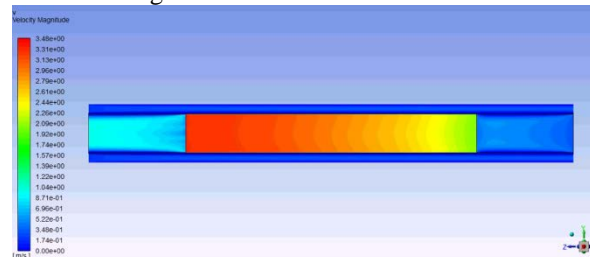


Fig. 4. Velocity magnitude distribution of the tubular steam methane reformer.

In the case of Fig.2, the porosity is set to 50% and the pre-exponential factors of chemical reactions are adjust to fit a commercial catalyst for validation. The simulation results is in consistent with the experiment results. To further analyze the effect of

simulation parameters of the catalyst model, two other simulation case with different pre-exponential factor and the porosity are carried out. The comparison of three studied cases are listed in Table 1. The case 2 with a higher pre-exponential factor performs almost totally methane reforming and over 87% hydrogen production rate. The mole fraction distribution in Fig.5 shows the methane reforming rate is faster than that in Fig. 3. The other case 3 presents the effect of porosity on the reforming rate. The simulation results show that the catalyst bed with a small porosity might restrict the methane reforming and hydrogen production. The results in Table 1 represents the present numerical model of steam methane reforming has enough accuracy and is suitable for different catalyst beds. According to the characteristics of catalysts, specific parameters of the simulation model can be confirmed and applied.

Table 1. Methane reforming performance of different simulation parameters.

Parameters and Methane reforming performance	Case 1 (Original)	Case 2	Case 3
Porosity (%)	50	50	25
Pre-exponential factor ( $cm^3/mol/s$ )	$1.0 \times 10^8$	$3 \times 10^8$	$1.0 \times 10^8$
CH <sub>4</sub> reforming rate (%)	93.44	99.13	91.35
Hydrogen production rate (%)	79.48	87.46	77.45
CH <sub>4</sub> mole fraction of reforming gases(%)	1.57	0.19	2.11
H <sub>2</sub> mole fraction of reforming gases (%)	76.07	77.77	75.60
CO mole fraction of reforming gases (%)	13.37	10.38	13.57
CO <sub>2</sub> mole fraction of reforming gases (%)	8.99	11.66	8.72

#### Temperature effect on the reforming gases

To investigate the temperature effect on the methane reforming process, Table 2 shows the simulation results of methane reforming at different inlet fuel temperature of 500°C, 600°C and 700°C. To magnify the effects, the pre-exponential factor of steam-methane reforming reaction is reduced by an order of magnitude. Besides, the pre-exponential factor of water-gas-shift reaction is simultaneously increased by an order of magnitude to further investigate the effects of the simulation parameters. As

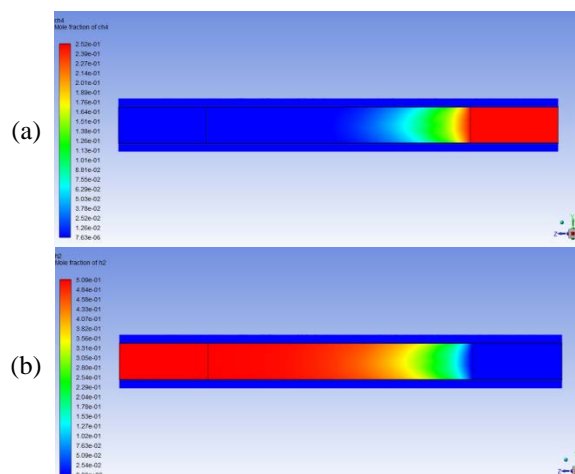


Fig. 5. Mole fraction distribution of (a) CH<sub>4</sub> and (b) H<sub>2</sub> of the tubular steam methane reformer at a higher pre-exponential factor.

Table 2. Methane reforming performance of different inlet fuel temperature.

Parameters and Methane reforming performance	Study cases		
	500	600	700
Inlet fuel temperature (°C)	500	600	700
CH <sub>4</sub> reforming rate (%)	62.94	78.85	86.54
Hydrogen production rate (%)	61.74	77.82	85.75
CH <sub>4</sub> mole fraction of reforming gases (%)	10.68	5.14	3.04
H <sub>2</sub> mole fraction of reforming gases (%)	71.18	75.69	77.43
CO mole fraction of reforming gases (%)	1.39	1.00	0.71
CO <sub>2</sub> mole fraction of reforming gases (%)	16.75	18.17	18.82

the results in Table 2, both CH<sub>4</sub> reforming rate and hydrogen production rate are smaller than that of the cases in Table 1. However, the transformation rate of carbon monoxide into hydrogen increases. A few CO mole fraction are found in the reforming gases. The results present the ability of the numerical model in this study for fitting the characteristic parameters of studied catalysts.

Generally, high reaction temperature is benefit to steam methane reforming process. The results in Table 2 shows that the CH<sub>4</sub> reforming rate by inlet fuel gases at 700°C is 37% larger than that by inlet fuel gas at 500°C, while the hydrogen production rate is of 39%

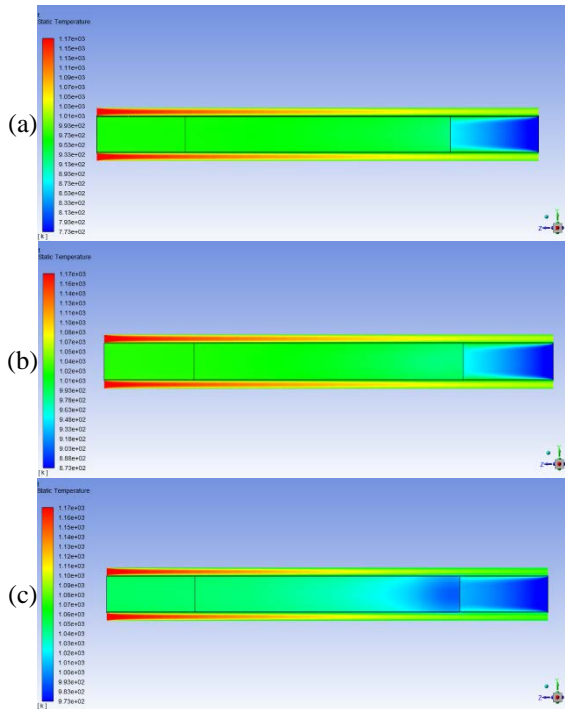


Fig. 6. Temperature distribution of the tubular steam methane reformer of inlet fuel gases at (a) 500°C, (b) 600°C and (c) 700°C.

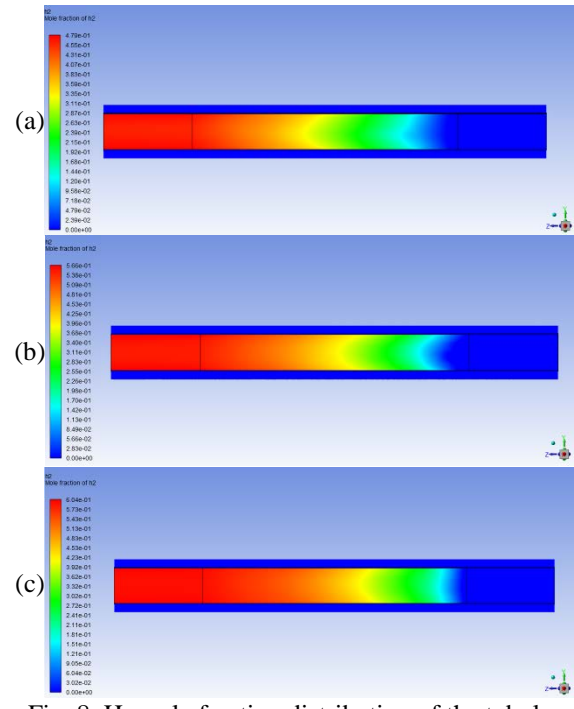


Fig. 8. H<sub>2</sub> mole fraction distribution of the tubular steam methane reformer of inlet fuel gases at (a) 500°C, (b) 600°C and (c) 700°C.

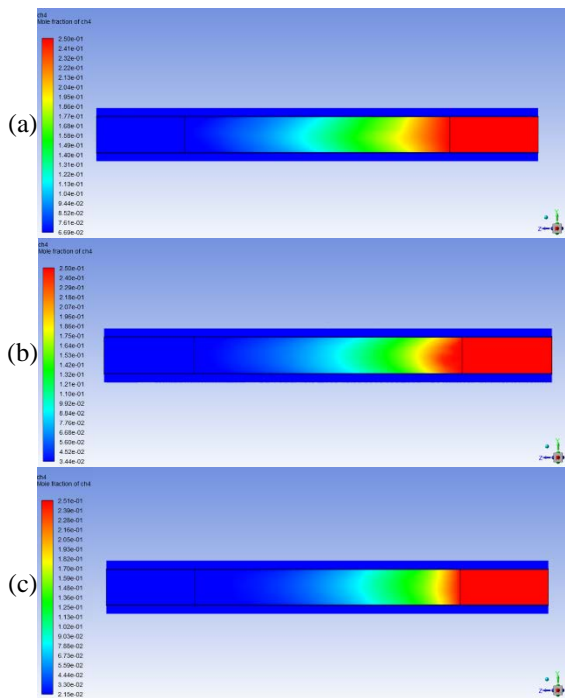


Fig. 7. CH<sub>4</sub> mole fraction distribution of the tubular steam methane reformer of inlet fuel gases at (a) 500°C, (b) 600°C and (c) 700°C.

increase as the inlet fuel temperature increases. The comparison of temperature distribution, CH<sub>4</sub> and H<sub>2</sub> mole fraction distributions are shown in Figs. 6-8. It shows that higher inlet fuel temperature would accelerate the steam methane reforming reaction and certainly contribute to the methane reforming performance.

### CONCLUSIONS

In this study, the numerical model of steam methane reforming in a tubular catalyst bed is proposed. The governing equations of mass transport, chemical reactions, and conjugated heat transfer in a tubular steam methane reformer are solved by the computational fluid dynamics. The heat required in the endothermic reforming process is provided by the heat exchanger with a double-pipe configuration. The performance of the steam methane reformer is investigated by monitoring the spatial temperature distributions and the reformat compositions in the processor. The numerical model includes the material parameters related to the characteristics of catalysts. In the study cases of the present work, the effect of various simulation parameters on the methane reforming performance is discussed as well as the effect caused by the temperature of inlet fuel flows.

By adjusting the parameters of the simulation model to fit a commercial catalyst, the calculated methane reforming rate and hydrogen production rate give a good agreement with the experimental data. The simulation pressure drop is also fitted to the

experimental value within a range of 1.8~2.2 mbar. The temperature distribution show a considerable thermal gradient between the side wall and the center of the bed, which was mentioned in literatures and observed in the experiments. The simulation results by various parameters show the present model is suitable for different catalysts. In the study cases, the calculated methane reforming rates are ranged from 63% to 99% with the hydrogen production rate in the range of 62%~87%. Besides, the reaction rates of steam methane reforming and water-gas-shift reaction are adjustable in the simulation model. The results in this study shows that the present numerical model of steam methane reforming has enough accuracy and is suitable for different catalyst beds. According to the characteristics of catalysts, specific parameters of the simulation model can be confirmed and applied.

### ACKNOWLEDGEMENT

We gratefully appreciate the financial support from the Bureau of Energy (BOE), Ministry of Economy Affairs (MOEA), Taiwan (Grant number: 108-D0901).

### REFERENCES

- Bayat, M., Rahimpour, M.R., Taheri, M., Pashaei, M., Sharifzadeh, S., "A comparative study of two different configurations for exothermic-endothermic heat exchanger reactor," *Chem Eng Process*, Vol. 52, pp. 63-73, 2012.
- Blazek, J., *Computational Fluid Dynamics: Principles and Applications*, Elsevier Science, New York, 2001.
- Cheng P., "Two-dimensional radiating gas flow by a moment method," *AIAA Journal*, Vol. 2, pp. 1662-1664, 1964.
- European Commission EU. *Energy Roadmap 2050*; European Commission EU: Brussels, Belgium, 2011.
- Fukuhara, C., Igarashi, A., "Performance simulation of a wall type reactor in which exothermic and endothermic reactions proceed simultaneously, comparing with that of a fixed bed reactor," *Chem Eng Sci*, Vol. 60, pp. 6824-6834, 2005.
- Lauder B. E., Sharma B. I., "Application of the energy dissipation model of turbulence to the calculation of flow near a spinning disc," *Letter in Heat and Mass Transfer*, Vol. 12, pp. 131-138, 1974.
- Lee, S.H.D., Applegate, D.V., Ahmed, S., Calderone, S.G., Harvey, T.L., "Hydrogen from natural gas: part I-autothermal reforming in an integrated fuel processor," *Int J Hydrogen Energy*, Vol.30, pp.829-842, 2005.
- Jones W. P., Launder B. E., "The prediction of laminarization with a two-equation model of turbulence," *Int. J. Heat and Mass Transfer*, Vol. 15, pp. 301-314, 1972.
- Jones, W. P., Whitelaw, J. H., "Calculation methods for reacting turbulent flows: A review. *Combustion and Flame*," Vol. 48, pp. 1-26, 1982.
- Mei, H., Li, C.Y., Ji, S.F., Liu, H., "Modeling of a metal monolith catalytic reactor for methane steam reforming-combustion coupling," *Chem Eng Sci*, Vol. 62, pp. 4294-4303, 2007.
- Ni, C., Yuan, Z., Wang, S., Li, D., Zhang, C., Li, J., Wang, S., "Study on an integrated natural gas fuel processor for 2-kW solid oxide fuel cell," *International Journal of Hydrogen Energy*, Vol. 40, pp.15491-15502, 2015.
- Nijemeisland, M., Dixon, A.G., Hugh Stitt, E., "Catalyst design by CFD for heat transfer and reaction in steam reforming," *Chem. Eng. Sci.*, Vol. 59, pp. 5185-5191, 2004.
- Palma, V., Ricca, A., Martino, M., Meloni, E., "Innovative structured catalytic systems for methane steam reforming intensification", *Chemical Engineering & Processing: Process Intensification*, Vol. 120, pp. 207-215, 2017.
- Peng, X. D., "Analysis of the Thermal Efficiency Limit of the Steam Methane Reforming Process", *Ind. Eng. Chem. Res.*, Vol. 51, pp.16385-16392, 2012.
- Pret, M.G., Ferrero, D., Lanzini, A., Santarelli, M., "Thermal design, modeling and validation of a steam-reforming reactor for fuel cell applications, " *Chemical Engineering Research and Design*, Vol. 104, pp. 503-512, 2015.
- Ramaswamy, R.C., Ramachandran, P.A., Dudukovic, M.P., "Coupling exothermic and endothermic reactions in adiabatic reactors," *Chem Eng Sci*, Vol. 63, pp.1654-1667, 2008.
- Shayegan, J., Hashemi, M.M.Y.M., Vakhshouri, K., "Operation of an industrial steam reformer under severe condition: a simulation study," *Can. J. Chem. Eng.*, Vol. 86, pp.747-755, 2008.
- Sivathanu, Y. R., Faeth, G. M., "Generalized state relationships for scalar properties in non-premixed hydrocarbon/air flames," *Combustion and Flame*, Vol. 82, pp. 211-230, 1990.
- Zel'dovich, Y. B., Raizer, Y. P., "Physics of shock waves and high-temperature hydrodynamic phenomena," *Dover Publications*, Mineola, NY, 2002.

# 管式甲烷蒸氣重組器數值 建模分析

張勳承 楊証皓

工業技術研究院綠能與環境研究所

馮子軒 陳朝光

國立成功大學機械工程學系

## 摘要

甲烷蒸氣重組為產氫的主要方式之一，透過將富含碳氫燃料的氣體，如天然氣、生質氣體等進行化學重組反應，可獲得高含氫率之合成氣體。本研究建立管式甲烷蒸氣重組器之數值模擬模型，透過計算流體力學法來求解重組氣體之質能傳遞與化學反應方程式，以了解甲烷蒸氣重組過程之現象特性。藉由調整數值模型之特徵參數，本研究將重組模擬結果與商用觸媒實驗結果比較，可獲得一致的重組產氣比率，而重組器內部之溫度分布場模擬，亦與實驗結果以及相關文獻分析吻合。因此，本研究提出之甲烷蒸氣重組數值模型，具有足夠的準確度。本研究之數值模型可根據不同觸媒特性來進行特徵參數之擬合匹配，以確保模擬結果可與特定觸媒之性能吻合。在本研究的模擬特例中，根據不同觸媒參數之調控，甲烷轉化率可介於 63% 到 99% 之間，並獲得 62%~87% 之氫氣產生率，驗證數值模擬模型之可應用範圍大。